

Introduction

Sweden and Finland are planning to dispose of spent nuclear fuel in a deep underground repository constructed in granitic rock. Each country is investigating candidate sites and developing the scientific and technical basis for assessing the safety of an eventual repository. An essential part of the safety assessment involves understanding the behaviour of the spent fuel after it is placed in the geologic environment.

The fuel will be sealed inside a copper canister that contains a cast iron insert. The copper functions as a corrosion resistant barrier, while the cast iron insert fills much of the internal void space, adding strength to the canister and reducing the space available for water to accumulate inside the canister after the corrosion barrier is breached. The canisters will be surrounded by compressed bentonite, which will limit the access of water and dissolved species to the canister. Oxygen that is initially present when the disposal environment is sealed will be rapidly consumed by pyrite in the bentonite, bacterial species in the rock, and reduced inorganic materials in the rock.

The copper canister will prevent access of water to the iron until it is corroded through, a process that is expected to take millions of years. After water contacts the iron, anaerobic corrosion of the insert will generate hydrogen gas and introduce Fe(II) ions into the water. The long-term environment for the fuel, therefore, is a highly reducing environment. The only possible source of oxidising agents is radiolysis of the water by radiation from the fuel. In the long-term, the radioactivity in the fuel is due to isotopes that decay by alpha decay; most of the activity from beta and gamma radiation will have decayed away.

Spent fuel that is available for testing contains high levels of beta and gamma activity. Even when testing is done in the presence of hydrogen or actively corroding iron, the radiolysis due to beta and gamma radiation can introduce oxidising agents into the system that will not be present under long term disposal conditions. A simulation of long-term conditions can be done using uranium dioxide that contains a short-lived isotope of uranium, but this will not include the effects of fission product and higher actinide elements on the behaviour of the spent fuel.

We designed a project that had as its objective to improve the scientific understanding of the processes that control release of radioactive species from spent fuel inside a disposal canister and the chemical changes in those species that might limit release of radioactivity from the canister. If the mechanisms that control dissolution of the fuel matrix, including self-irradiation effects, can be clarified, a more realistic assessment of the long-term behaviour of spent fuel under disposal conditions can be made. By removing uncertainties concerning waste form performance, a better assessment of the individual and collective role of the engineered barriers can be made.

To achieve the overall objective of the project, the following scientific and technical objectives were set.

1. Measure the actual rate of matrix dissolution of uranium dioxide under oxidising and reducing conditions.
2. Measure the effect of alpha radiolysis on the dissolution rate of uranium dioxide under oxidising and reducing conditions.
3. Measure the dissolution rate of the matrix material of spent fuel and thereby determine the additional effects of beta and gamma radiation on uranium dioxide dissolution rate under oxidising and reducing conditions.
4. Measure the ability of actively corroding iron to reduce oxidised U(VI) to U(IV) when U is present as the complex ion uranyl carbonate.
5. Measure the rate of reduction of Np(V) species in the presence of actively corroding iron.
6. Calculate the expected equilibrium and steady state concentrations of U under the conditions of the experiments used for meeting objectives 1 through 3 and compare the calculated results with those measured in the experiments.
7. Calculate from first principles the expected reaction path, and the relative reaction rate for the reduction of U(VI) to U(IV) under the conditions of experiments used to meet objective 4 and with other ligands in solution. Similar calculations will also be done for reduction of Np(V) to Np(IV) for solutions with various ligands.

As the project progressed, item 6 was found to be unnecessary and item 7 was modified to the more specific task of calculating the reduction of U(VI) to U(V) by Fe(II) using ab initio methods.

Each of the technical and scientific objectives was a work package within the project. (Item 7 was WP6). The following summary will describe the principle results of each work package.

WP1

Dissolution rates of uranium dioxide under air atmosphere and actively reducing conditions

Tests were conducted using unirradiated fuel pellets and fragments of fuel pellets. The tests were done at ambient temperature in a synthetic low ionic strength groundwater similar in composition of that found in Scandinavian groundwaters. The composition of the groundwater used in air atmosphere tests is given in table 1. The composition for reducing conditions tests is given in table 2. This water is referred to as “modified Allard groundwater”. The modifications were done to insure stability of the solutions under the testing conditions.

Tests were conducted at AEA Technology Harwell using fuel pellets purchased from BNFL. These pellets contained 4.5% ^{235}U . Tests were also conducted at VTT using fuel pellets obtained from ABB that contained 2.8% ^{235}U . Tests were done using an isotope dilution method that allows calculation of the amount of sample that dissolves even if precipitation is also occurring. The tests are started with solutions that contain a spike of uranium that has an isotopic composition that is different from that in the solids. By measuring the concentration of U in the solutions and the isotopic composition of the solutions we can calculate how much U has dissolved and determine how much, if any, has precipitated.

$$\left(\frac{^{235}\text{U}}{^{238}\text{U}}\right)_{\text{measured}} = \left(\frac{^{235}\text{U}_{\text{initial}} + ^{235}\text{U}_{\text{dissolved}}}{^{238}\text{U}_{\text{initial}} + ^{238}\text{U}_{\text{dissolved}}}\right)$$

The tests were initially started at three different spiking levels using depleted U as the spike. The concentrations used were 0.5, 1.0, and 2.0 ppm. Each test used 1 gram of pellet fragments with size range 1.4 to 4 mm and 25 ml of solution. Details of the test procedure and all of the results are given in /Ollila et al, 2003/. Some tests at VTT used intact pellets with the amount of solution adjusted to give the same solid surface area to solution volume ratio.

Table 1. Composition for air atmosphere tests.

	(mg/L)	(mmol/L)
Na ⁺	52.5	2.3
Ca ²⁺	10.2	0.25
Mg ²⁺	2.8	0.11
K ⁺	3.9	0.10
SiO ₂	2.9	0.05
SO ₄ ²⁻	9.6	0.10
Cl ⁻	47.5	1.3
HCO ₃ ⁻	90.7	1.5
pH _{theoretical}	8.4	

Table 2. Composition for reducing conditions tests.

	(mg/L)	(mmol/L)
Na ⁺	52.5	2.3
Ca ²⁺	5.1	0.13
Mg ²⁺	0.7	0.03
K ⁺	3.9	0.10
SiO ₂	1.7	0.03
SO ₄ ²⁻	9.6	0.10
Cl ⁻	48.8	1.4
HCO ₃ ⁻	65.0	1.1
pH _{theoretical} (log pCO ₂ = -4)		8.8

Very early in the experiments it became apparent that the two different fuel pellet materials were dissolving at different rates, with the BNFL materials dissolving much slower than the ABB materials. This, combined with the lower enrichment level for the ABB materials meant that the solution had too much U that came from the fuel pellet and the spike was no longer useful. We terminated the initial VTT tests and restarted some of them in solutions with 7 and 10 ppm depleted U. During this time it also became apparent that the analytical laboratory used by AEA Technology was not able to produce reliable analytical data. Testing at Harwell was, therefore, terminated. Results for the first cycle of testing at VTT are shown in figure 1. The tests with fuel pellets are dissolving at a faster rate than those with fragments. Since both tests have the same geometric surface area to solution volume we believe this must be due to effects of porosity in the fuel pellets increasing the active surface area.

Results for the restarted VTT tests are shown in figure 2. The tests started at 7 ppm U have reached a steady-state [U] of about 9 ppm, while the test started at 10 ppm peaked at about 13 ppm and is decreasing. Results of the isotope dilution calculation for the two pellet tests are shown in figure 3. It is clear that both tests show evidence for precipitation of U. These tests will be continued to see whether they eventually reach the same steady-state solution concentrations.

Tests under reducing conditions were conducted at VTT. Details of the test procedures and all of the results are contained in the report by /Ollila et al, 2003/. All tests were conducted at ambient temperature in high-density polyethylene bottles using 50 ml of modified Allard groundwater with 1g of fragments or one intact pellet. The groundwater was pretreated by adding an Fe strip so that an equilibrium concentration of Fe(II) would be established before the water was contacted with the samples. The tests were conducted in a N₂ atmosphere glove box. Residual O₂ in the box was on the order of 0.1 ppm. All samples were analysed for [U] and isotopic composition of U by ICP-MS.

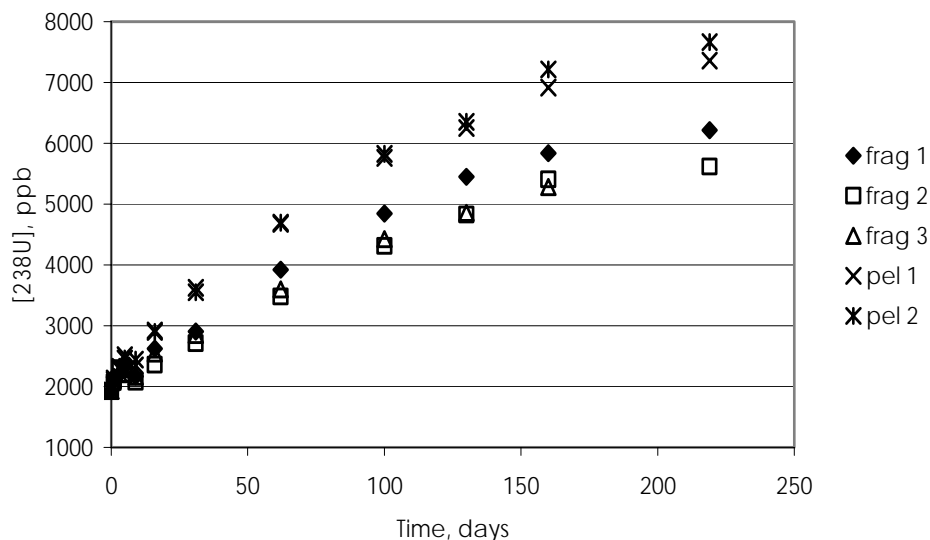


Figure 1. Results from testing of unirradiated fuel pellets and pellet fragments in modified Allard groundwater. Tests conducted at VTT.

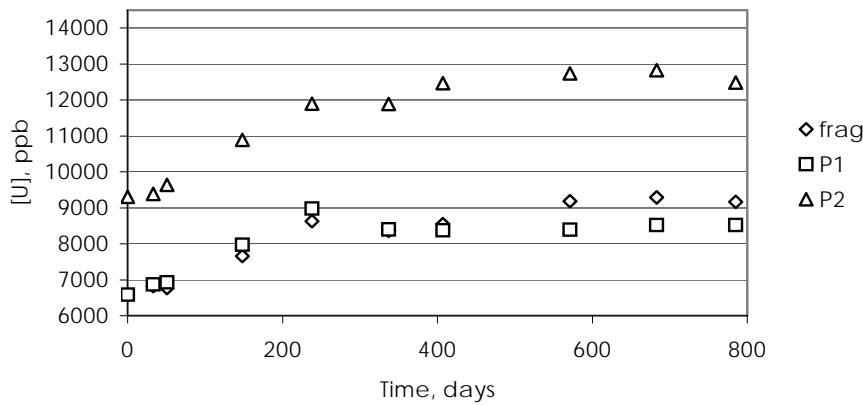


Figure 2. Data for restarted VTT tests with pellets and fragments for solutions in contact with air.

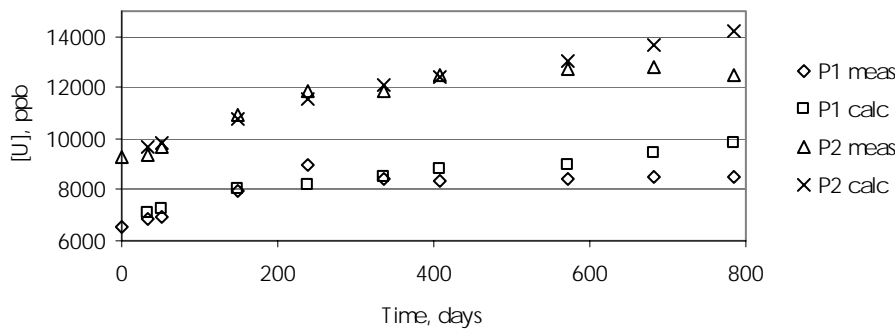


Figure 3. Comparison of measured $[^{238}\text{U}]$ and $[^{238}\text{U}]$ calculated from the isotopic ratio changes.

Samples were pretreated by contacting them with modified Allard groundwater in several successive steps. Then the samples were pretreated with groundwater and an Fe strip in two cycles with change of vessels between cycles. In the last pretreatment cycle the [U] in solution after 10 days was ≤ 0.1 ppb in all cases and the total amount of U recovered in solutions + vessel rinse + acid strip was about $0.6\mu\text{g}$ for fragment samples and $0.15\mu\text{g}$ for pellet samples.

Samples were tested using 50 ml of solution containing 0.08 or 0.12 ppb of U with an isotopic composition of $^{235}\text{U}/^{238}\text{U} = 0.978$. All tests contained an iron strip to produce actively reducing conditions. After one day of exposure the samples had (with 2 exceptions) [U] that was similar to what had been added as the spike. After 7 days of testing all samples except one had $[\text{U}] < 0.02$ ppb (the detection limit for ^{238}U); one sample had 0.04 ppb ^{238}U . After 14 days the tests were terminated. All samples had $[\text{U}] < 0.02$ ppb. Vessel rinse solutions contained low amounts of U (10 to 35 ng) with an isotopic composition indistinguishable from that of the solid. Acid stripping of the vessels yielded 40 to 580 ng U, again with isotopic composition indistinguishable from the solid.

To improve the sensitivity of the tests the next series of testing used a spike with $^{235}\text{U}/^{238}\text{U} = 10.354$. Four tests with fragments and 2 with pellets were done with the Fe strip in the test. Four tests with fragments were done without the Fe strip. Samples were taken after 47 days of testing. Those tests that contained an Fe strip had $[\text{U}] < 0.02$ ppb (except for one test with 0.03 ppb), while the fragment tests without Fe had U between 0.1 and 0.85 ppb U. For the two samples that had the highest concentration of spike (0.1 ppb U added), it was possible to show the even without the Fe strip, 40% of the spike had precipitated in one case and 83% in the other. The total sample solution was removed from the solids and acidified. These samples all showed measurable $[\text{U}]$. For tests with the Fe strips, the $[\text{}^{238}\text{U}]$ ranged from 0.26 ppb to 1.92 ppb; however, the isotopic composition was the same as the starting solid, indicating that small grains of sample had been dislodged when the total solution was removed. The acidified solution samples for tests conducted without Fe strips showed $[\text{}^{238}\text{U}]$ slightly higher than the original samples and with decreases in the $^{235}\text{U}/^{238}\text{U}$ ratio indicative of dissolution of new solid.

The next series of tests investigated the effect of test duration on results. Batch tests of 1, 2, 4, and 8 weeks duration were conducted with the fragment samples from the previous tests. Tests were started in solution with an Fe strip and allowed to run for 2 days before addition of the spike. This was to allow any initial pulse of U release due to contact with air during sample changes to precipitate. Measured $[\text{}^{238}\text{U}]$ before addition of the spike ranged from 0.02 ppb to 0.11 ppb for 7 of the samples and was 0.46 ppb for the remaining sample. From these concentrations and the amount of spike added, an expected isotopic composition for the solution can be calculated. Samples were taken after one day of exposure with the spike. The measured $^{235}\text{U}/^{238}\text{U}$ ratio was compared with that expected if the day 2 $[\text{U}]$ had been representative of the U in true solution. The measured $^{235}\text{U}/^{238}\text{U}$ ratio was in all cases higher than that calculated assuming a homogeneous solution with $[\text{U}]$ as measured at day 2. This means that the solutions at day 2 were not homogeneous and that the measured samples at day 2 contained colloidal material that did not equilibrate with the spike. The concentrations of ^{238}U measured at day 3 were between 0.04 and 0.07 ppb, indicating that the colloidal material had precipitated. Calculation of the isotopic composition that would result from mixing the measured amount of ^{238}U at day 3 with the added spike gave good agreement with the measured values in 5 cases and a higher ratio in 3 cases. A calculated ratio higher than the measured ratio means that some of the U that was in true solution at day 2 (sample + spike) has precipitated. Samples taken after 2 further days in the spiked solution (Day 5 of the test) showed lower $[\text{U}]$ than the Day 3 samples, but the same isotopic composition, indicating that the solution now had a homogeneous distribution of U (no colloids) and that precipitation was occurring.

At test termination after 1 week, one sample contained 0.03 ppb ^{238}U and the other was below detection limits, < 0.02 ppb. The sample with 0.03 ppb had isotopic composition indistinguishable from that measured at day 3 and day 5, indicating no further dissolution of solid occurred. Solution samples at longer testing times all were < 0.02 ppb. The analysis of the remainder of the solution after removal from the solid and acidification with a holding time of 3 to 6 days showed again evidence that small grains of UO_2 were dislodged from the sample when the solution was removed. The amounts of U found were very small, consistent with 1 or 2 grains with dimensions of 5 to 7 μm .

The final test series under reducing conditions was designed to eliminate the effects of any “puff” of U released at the start of a test. The underlying thought behind the “puff test” procedure was to protect the sample using a relatively thick layer of solution. Two samples of fragments from the previous tests were transferred to new reaction vessels and 50 ml of conditioned water was added. The tests were allowed to equilibrate for 2 hours, during which time we hoped that any oxidised material would dissolve. After the 2 hours, 30 ml of solution was removed and replaced with new conditioned water. The solution was stirred, covered, and left for 30 minutes. This dilution step was repeated 2 more times. Then the spike was added, as well as an Fe strip, and the test was covered and left for one day before sampling.

We were surprised to see that neither of the samples showed an initial pulse of U release. Perhaps the sample transfer was faster since only two samples were being handled and the access to oxygen was less. Samples taken after 1 day of exposure had 0.03 and 0.06 ppb ^{238}U and had $235/238 = 8$. The isotopic composition indicates that the $[\text{}^{238}\text{U}]$ before spike addition was 0.01 ppb. Samples after 4 days with the spike had $[\text{}^{238}\text{U}] \leq 0.02$ ppb. The sample with $[\text{}^{238}\text{U}] = 0.02$ ppb had $235/238 = 7.6 \pm 1.0$, showing no additional sample dissolution had occurred between day 1 and day 4. Solution samples at day 7 and termination at day 14 were all < 0.02 ppb. The amount of ^{235}U recovered in acidified solutions at test termination was only about 2% of that added as spike. Vessel rinse solutions were consistent with small amounts of sample grains, with isotopic composition close to that of the solid. The acid strip of the vessel was also dominated by material with isotopic composition close to the solid, but did contain about 10% of the ^{235}U that had been added as spike.

Taken as a whole, these tests showed that the presence of an Fe strip in the test solutions was capable of producing highly reducing conditions under which the solubility of UO_2 is very low - < 0.02 ppb, corresponding to $< 4 \times 10^{-11}$ M. The $[\text{U}]$ predicted for solubility of UO_2 in modified Allard groundwater at $\text{Eh} = -0.25\text{V}$ using published solubility and other thermodynamic data /Ollila, 1999/ is an order of magnitude higher than found in these experiments. This suggests that a re-evaluation of the published data is needed.

WP2

Dissolution rates of unirradiated UO_2 fuel pellet material doped with ^{233}U

The purpose of the tests done in this work package was to assess whether the presence of significant amounts of alpha activity in the samples would increase the dissolution rate of the solid. Samples containing 4.5% ^{235}U and 5% or 10% ^{233}U were prepared by BNFL. Details of the samples are given in /Ollila et al, 2003/. A limited amount of testing was done at Chalmers Technical University under air atmosphere to determine whether these experimental pellets behaved in a manner similar to BNFL commercial fuel pellets (used in WP1 tests at AEA Technology). Testing followed the procedures used in WP1 except that glass vessels were used instead of plastic. Fragments of 1.4 to 4 mm size were used. Triplicate samples were tested of each doping level and also of a control sample of depleted U fuel. Analyses were performed by ICP-MS. Pretreatment of the doped samples gave isotopic compositions for the leaching solutions that showed that the actual composition of the solids was probably 4.3% ^{235}U and 4.8% or 9.6% ^{233}U , somewhat lower than the target levels.

The tests were conducted using a starting $[\text{U}]$ of 1.5 ppm depleted U (0.2% ^{235}U). Data for the three 5% ^{233}U -doped samples showed generally more variability between samples than the 10% ^{233}U -doped samples. The results for the 5% samples are shown in figure 4, in which clear differences in total $[\text{U}]$ can be seen for the last two sampling times. A similar plot for the 10% samples would show all three samples plotting on top of each other.

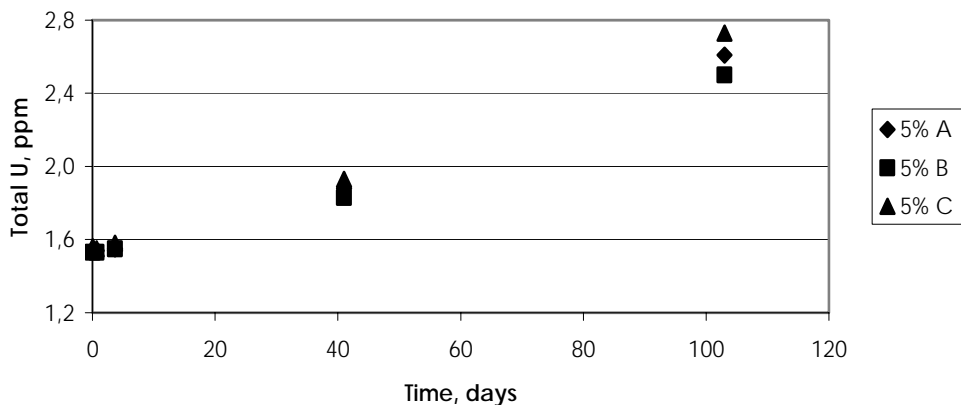


Figure 4. Total $[\text{U}]$ for samples with 5% ^{233}U -doping tested in modified Allard groundwater in contact with air atmosphere.

Figure 5 shows a comparison of the results for [U] in solution for the three different sample types. At this stage, the samples with 10% ^{233}U -doping seem to be dissolving at a somewhat faster rate than those with the 5% ^{233}U -doping. For testing under an air atmosphere, one would not expect to see any effects from the alpha radiolysis in solution on dissolution rates. We, therefore, suspect that differences in the quality of the pellets – i.e., the level of defects in the materials – may be the cause of the dissolution rate differences. These materials will be studied further in the future. Despite the slight differences in the dissolution rates, the general level of the [U] and the rate of increase of [U] indicate that the pellets are of adequate quality.

For the sample with nominal 5% doping, an isotope dilution calculation based on the 103 day data and the $^{233}\text{U}/^{238}\text{U}$ ratio indicated that 1.08 ppm total U has dissolved since the spike was added. This converts to a predicted solution concentration of 2.65 ppm total U, which is in excellent agreement with the average measured value of 2.61 ppm. A similar calculation based on the $^{235}\text{U}/^{238}\text{U}$ ratio indicates that 1.41 ppm U has dissolved. If the actual composition of the solid was $^{235}\text{U} = 4.5\%$, the calculated amount of dissolution would be 1.29 ppm. Both of these values are higher than the dissolution calculated from the $^{233}\text{U}/^{238}\text{U}$ ratio and may indicate that the solids are inhomogeneous. This will be examined further in the future.

An isotope dilution calculation for the 10% sample based on the 103 day data and the $^{233}\text{U}/^{238}\text{U}$ ratio indicates that 2.60 ppm U should have dissolved since the addition of the spike. This amount of U together with the spike and the 0.1 hour sample would give an expected [U] of 4.2 ppm. This is considerably higher than the average of the measured values, 3.59 ppm. If the isotopic composition of the solid is estimated using the data from the 0.1 hour sample, the indicated dissolution increases to 2.80 ppm. Thus, the indications for precipitation occurring during the 103 day period are strong. The calculation of dissolution using the $^{235}\text{U}/^{238}\text{U}$ ratio indicates dissolution of 3.06 ppm total U. Using the data from the 0.1 hour sample to predict the isotopic composition for the solid for ^{235}U (4.15%) would result in a higher calculated value. Using the nominal value of 4.5% gives a calculated dissolution of 2.7 ppm, which is close to the value calculated from the $^{233}\text{U}/^{238}\text{U}$ ratio. In any case, all calculations indicate that precipitation has occurred from the 10% ^{233}U tests. Before any stronger conclusions can be reached, we must resolve the issue of establishing the isotopic composition of the solids and the degree of heterogeneity of the solids.

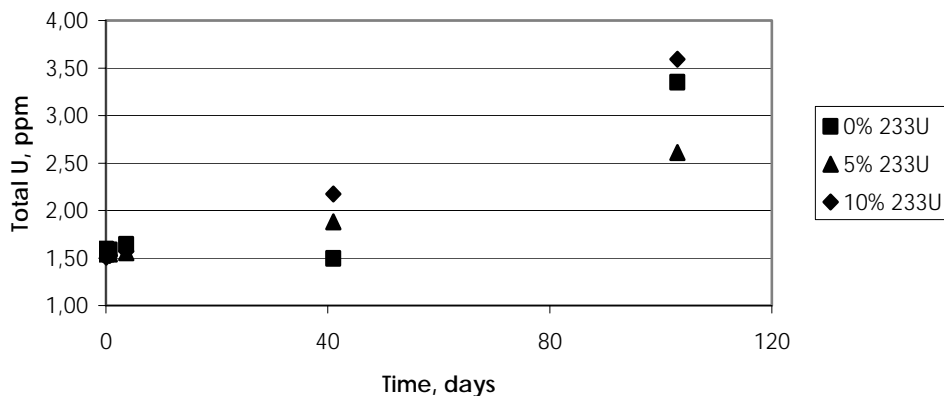


Figure 5. Solution concentration for U for the average of three samples at each doping level for tests in modified Allard groundwater in contact with an air atmosphere.

Tests under reducing conditions were done at VTT using a new, negative pressure anaerobic glove box. Duplicate samples of about 1 g each were prepared for each doping level plus a control sample of material similar to that used in WP1. Samples were pretreated as for the WP1 reducing conditions tests with several soakings in modified Allard groundwater, followed by two 1-week treatments that included an Fe strip and a final 17 day treatment. Data for the samples and details of the procedure are given in /Ollila et al, 2003/. The final solution samples were all < 0.02 ppb, as were two of the acidified remainder samples. The other acidified remainder samples showed 0.02, 0.10, 0.13, and 0.39 indicating good preparation of the sample surface had been achieved and that the solution residues had been separated from the solids without too much disruption of the solid surface.

All testing used a method based on the “puff test” procedure developed in the last stage of WP1. Details of the procedures and all analytical data are given in /Ollila et al, 2003/. Samples from the first dilution steps were analysed as “normal” samples and again after storage in acid for 1 and 2 weeks. The results showed generally low levels of U (< 0.1 ppb, with 4 exceptions, 3 of which were for the undoped samples). Analyses of the acidified remainder solutions were generally lower than the [U] found in the first sample suggesting that the original solutions were heterogeneous. Samples taken immediately after adding the ^{235}U spike showed $^{235}\text{U}/^{238}\text{U}$ ratios of about 8, indicating very low [U] before the spike was added. Samples were then taken after 1, 4, 7, and 14 days total exposure time. All samples had measurable U in the 1, 4, and 7 day samples and had changes in $^{235}\text{U}/^{238}\text{U}$ ratio that suggested that the 10% sample was reacting faster than the 5% sample, which was reacting faster than the undoped sample. At test termination, two samples – one each of the 5% and 10% doping levels – had [U] < 0.02 ppb. The remaining 4 samples had measurable U and $^{235}\text{U}/^{238}\text{U}$ ratios that indicated that dissolution had continued during the last week of testing, even though the [U] in solution at termination for the undoped samples showed that precipitation had occurred during the last week of testing.

The samples were transferred to new reaction vessels and the puff test procedure was repeated. The dilution steps all showed similar amounts of U, indicating that fairly rapid dissolution of small amounts of U (about 0.2 ppb) was occurring for all samples. A spike dose was added to provide an increase of 0.4 ppb U to the solutions. The amount of ^{235}U calculated to be in solution based on the measured [^{238}U] and the $^{235}\text{U}/^{238}\text{U}$ ratio of the solutions measured after spike addition is consistent with the amount of spike added, which contained 0.365 ppb ^{235}U . The measured [^{238}U] in all samples except one of the 5% doping samples was higher than the expected value based on dilution of the residual 20 ml of solution from the sample 3 stage and addition of spike, indicating that even in the time frame of a few minutes, further dissolution was occurring. Samples taken after 1, 3, and 3 further days of exposure of the solids to modified Allard groundwater showed (by small changes in the $^{235}\text{U}/^{238}\text{U}$ ratio) that further dissolution was occurring and with a slight indication that the ^{233}U -doped samples were dissolving faster than the undoped samples.

The remainder of the solution from cycle 2 (25 ml) was transferred to a new reaction vessel together with the solid samples on their saucers and the Fe strip. The volume was increased to 50 ml and a new dose of spike was added to give an addition of 0.4 ppb total U to the system. The solution was gently mixed and a 5 ml sample taken for analysis. We can use the data from the 14 day test termination and the amount of spike added to calculate the expected results for these analyses. Table 3 shows the results of

Table 3. Cycle 2 restart after 14 days with new spike addition, day 14+0 samples. Sample 1–10 is the first sample of 10% ^{233}U .

Sample ID	Predicted ^{238}U , ppb	Measured ^{238}U , ppb	Predicted 235/238	Measured 235/238
1–10	0.25	0.27	2.11	2.18
2–10	0.22	0.22	2.48	2.69
1–5	0.215	0.22	2.53	2.81
2–5	0.30	0.31	1.89	2.06
1–0	0.125	0.15	3.82	3.72
2–0	0.10	0.17	4.10	3.58

these calculations and the measured values. The agreement between predicted and measured results is excellent.

The tests were left to equilibrate and samples were taken after 1, 3, 3, and 7 days of additional testing. The day 14+1 samples show the same isotopic composition as the 14+0 samples, indicating that no further dissolution has occurred. In addition, the concentrations of all samples had decreased, indicating active precipitation. At 14+4 days, three samples had ^{238}U less than the detection limit of 0.02 ppb. The other 3 samples had very low ^{238}U and the same isotopic composition (within the limits of uncertainty) as the day 14+1 samples, again showing that precipitation was occurring without further dissolution of the solids.

All samples taken at days 14+7 and 14+14 had $[^{238}\text{U}] < 0.02$ ppb. At day 14+15 a new dose of spike was added to each of the samples and a 5 ml sample was taken. The measured data for day 14+15 confirm that the $[^{238}\text{U}]$ at day 14+14 had been low, since the measured amount of ^{238}U at day 14+15 is consistent with the amount added with the spike. The isotopic composition of the solution after spike addition (8.7 to 10.2) is very close to the spike value. A measured value of $235/238 = 9$ after spike addition would correspond to an original $[^{238}\text{U}]$ before spike addition of 0.0056 ppb and $[^{238}\text{U}] = 0.0406$ ppb after spike addition.

The samples were left for an additional 7 days and then the tests were terminated. All tests had $[^{238}\text{U}] < 0.02$ ppb, both in an unfiltered acidified sample and in the remainder of the solution, which was analysed after 10 days equilibration with the acid. Extreme care was taken when the remainder of the solution was removed from the solid not to come in contact with the contents of the sample saucer. This seems to have enabled the solution to be removed without dislodging grains from the sample surfaces. The vessel rinse samples had low $[^{238}\text{U}]$ and accounted for recovery of about 1% of the added spike in the highest case (sample 2-0). The acid strip samples all had significant $[^{238}\text{U}]$ and isotopic compositions that were different from the starting solid. If the ^{235}U recovered is interpreted as all coming from precipitation of the spike, the amount in the acid strip amounts to 60% recovery for sample 1-10, 44% for sample 2-10, 50% for sample 1-5, 41% for sample 2-5, 68% for sample 1-0, and 93% for sample 2-0.

At the end of the test termination, the Fe strips were removed from the glove box and exposed to air for several hours. They were then immersed in 25 ml NaHCO_3 solution (250 ppm bicarbonate) in an attempt to remove any U that might be on the strips. This procedure was repeated twice more for a total of 3 successive strippings. Data for analysis of these solutions is in /Ollila et al, 2003/. The first stripping of the Fe strips from the ^{233}U -doped samples gave small amounts of U with a 235/238 ratio that was not far from what had been measured in the early stages of the restarted cycle 2 tests. This

indicates that the U came from the solution phase and precipitated onto or was reduced onto the surface of the Fe. Sample 1–5 indicates the largest recovery of spike U, corresponding to about 5% of the added spike. The second and third strippings gave [^{238}U] near or below detection limits and $^{235}\text{U} < 0.02$ ppb in all cases.

The results of the testing of ^{233}U -doped uranium dioxide pellet fragments under reducing conditions show only small effects in the early test cycles that might be attributed to the presence of alpha activity in the samples. Further testing is needed to determine whether the effects that are seen in early testing are due to alpha activity or due to differences in the quality of the samples. The last test cycle showed no effects that could be attributed to alpha radiolysis.

WP3

Dissolution rates of spent fuel under reducing conditions

The purpose of these tests was to provide results of dissolution under reducing conditions together with the full radiation field from spent fuel. This allows radiolysis effects from beta and gamma radiation as well as alpha.

The tests using spent fuel were originally planned to be done at AEA Technology, Harwell, using their hot cell facilities. In that location, we could have used the same experimental procedure as was used for tests with unirradiated fuel pellet materials and the alpha-doped materials. When it was announced that the hot cells would be closed before our experiments could be done, we had to relocate the tests. Fortunately, Chalmers was able to do the work, but with a revised experimental procedure that would use steel test vessels to provide some of the shielding needed when working with highly radioactive spent fuel.

The fuel samples used in the experiments at Chalmers came from a fuel pin from the Oskarshamn Nuclear Power Station (fuel pin OI-418-A6). The fuel pin had a burnup of 41 MWd/kgU. The samples were taken about 1 m from the bottom of the fuel pin and were originally used in an experiment involving 200 days of leaching in the presence of bentonite clay. Data from that and related experiments have been published as part of a diffusion study of fission products and actinides in bentonite clay /Albinsson et al, 1990, Ramebäck et al, 1994/. The leaching in the bentonite experiments should have removed most of the rapid release fraction of ^{137}Cs .

To prepare the samples for the isotope dilution tests, a series of experiments were done in a project outside of the EU Project. Before use in those experiments, the samples were removed from their cladding, at which time the samples separated into small fragments. The experiments used 2 fragments in each test, with a total weight of spent fuel of 0.4 to 0.6 g/test sample. The samples were rinsed and preleached to remove any traces of bentonite from the previous testing.

The spent fuel tests were conducted in steel vessels lined with PEEK (polyether ether ketone), a material that is non-reactive under the conditions used in our tests. The vessels are capable of withstanding significant gas pressures inside them during testing. The fluid phase used for the leaching is the modified Allard groundwater for reducing conditions. Tests were conducted under ambient hot cell temperature (18–25°C). The first cycle of testing used an argon atmosphere of 10 bar in the vessels. Samples were taken after 1, 4, 8, and 21 days of leaching. The atmosphere in the vessels was then changed to H_2 (10 bar) and an additional 20 ml synthetic groundwater was added to return the volume to approximately 30 ml.

Samples were again taken after 1, 3, 8, and 21 days. At the end of this cycle, the water was removed and replaced with groundwater that had been equilibrated with an Fe strip and an H_2 (10 bar) atmosphere. This gives a concentration of Fe(II) in the solution of approximately 1-0.1 μM . The change of solution was done in a hot cell with an air atmosphere. Another cycle of samples at 1, 4, 8, and 24 days was taken and the test was terminated.

The spent fuel samples were then transferred to new PEEK vessels for further testing. The vessels from the terminated test series were rinsed with groundwater and then stripped with nitric acid to recover any precipitated material. The test cycle with Fe-equilibrated water and H₂ atmosphere was repeated, including vessel changes, 3 more times. The change of vessel after sample number 20 (110 days total testing) was done in an Argon atmosphere box. The following analyses were done on each sample: ⁹⁰Sr via solvent extraction followed by Cerenkov counting of Y daughter product /Ramebäck et al, 1995/, Cs and Co using a HPGe-detector for gamma detection, and Fe, Sr, Mo, Tc, Ru, Np, U, Pu, and Zr by ICP-MS. Zr was below detection limits (5×10^{-11} M) in all samples. Measurement of pH shows that the presence of H₂ in the system did not affect the pH. Full data for these experiments are reported in /Albinsson et al, 2003/.

Data for U are shown in figure 6. In the Ar atmosphere, [U] increased from about 1×10^{-7} M after 1 day of leaching to about 1×10^{-6} M after 21 days of leaching. After changing to the H₂ atmosphere, the [U] began to slowly decrease. Changing the solution at day 42 produced a sharp increase in [U] to 1×10^{-5} M, probably due to some oxygen contacting the sample during the change of solution. By day 3 of the cycle with H₂ atmosphere and Fe(II) in solution, the [U] had dropped dramatically. The [U] continued to decrease during the rest of the cycle and at day 66 it was $\leq 1 \times 10^{-8}$ M. Subsequent changes of vessel and solution produced slightly elevated [U] at the start of the cycle, but none as dramatic as that for the start of cycle 3. The test termination at day 66 included rinsing and stripping of the reaction vessel. In test series 2 and 3, the total U recovered in the rinsing and acid stripping of the PEEK vessels was 2×10^{-9} moles U and 0.6×10^{-9} moles U respectively. The total U in solution at day 1 of the cycle was about 2×10^{-7} moles U. Thus, at most 1% of the uranium that had been in solution was recovered in the cycle termination. This indicates that the U that was precipitated from solution was taken up by the spent fuel sample itself, rather than precipitating or sorbing onto the vessel walls.

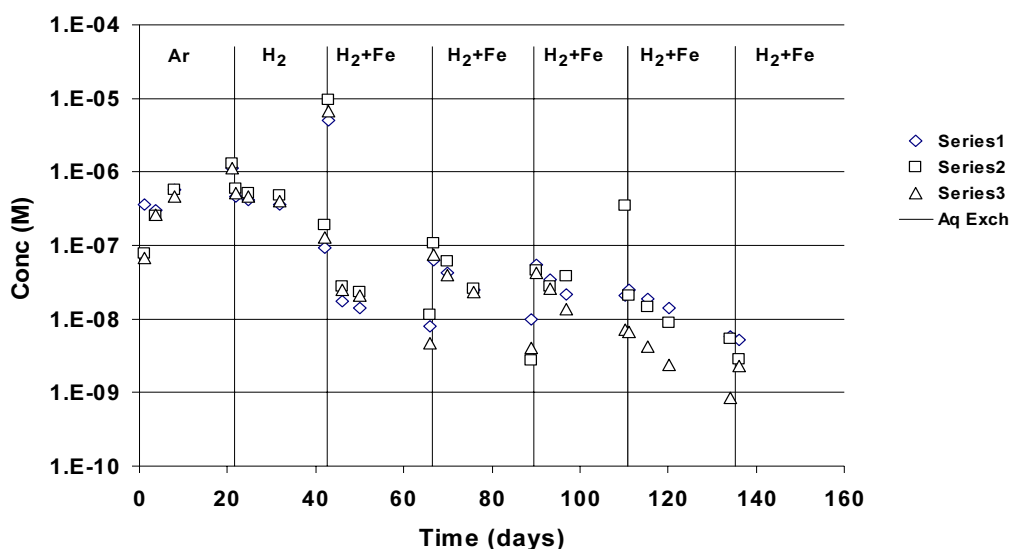


Figure 6. Leaching data for U. ICP-MS measurement.

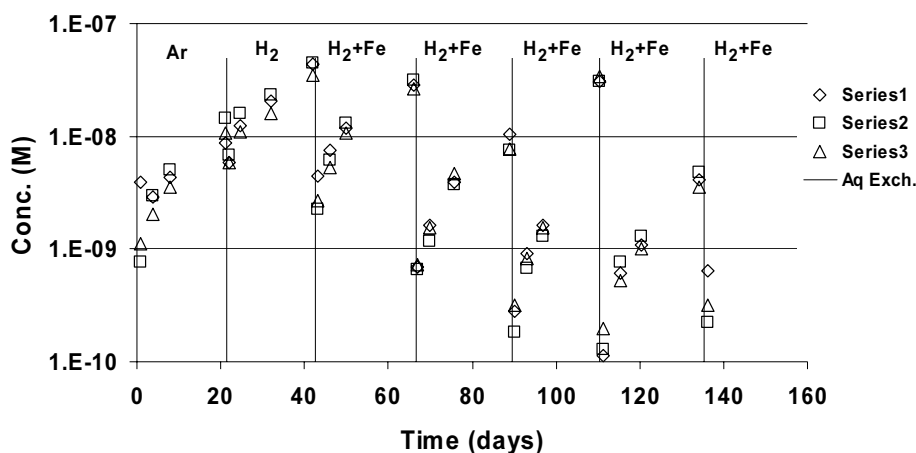


Figure 7. Leaching data for ^{137}Cs . Gamma measurements.

Data for ^{137}Cs are shown in figure 7. The small decrease in concentration at the change from Ar to H_2 atmosphere is the result of adding 20 ml of new groundwater to the tests to return the solution volume to near its original value. Each change of solution (day 42) and solution plus reaction vessel (days 66, 89, 110) resulting in exposure of the fuel to a new solution, started a new cycle of ^{137}Cs leaching. The release of ^{137}Cs during the first day of the 4 cycles with Fe(II) solutions seems to be getting lower in subsequent cycles, but there is no clear trend indicating a response to the reducing conditions on the ^{137}Cs release.

Strontium-90 concentrations ranged between 10^{-10} and 2×10^{-9} M, see figure 8, with the low values at the start of the leaching cycles. There is no dependence of $[\text{}^{90}\text{Sr}]$ on dissolution conditions. There was no spiked release of ^{90}Sr in the sample that showed the high $[\text{U}]$. The ^{90}Sr inventory in the fuel is about 0.04% of the sample by weight, while the ^{137}Cs is about 0.09% by weight.

We can use the ^{90}Sr data to calculate how much of the spent fuel U we would expect has been processed through the solution phase. The Sr is thought to be in solid solution in the UO_2 matrix /Kleykamp, 1985/, so release of Sr should indicate dissolution of spent fuel. The first samples of each of cycles 3 to 6 have $[\text{}^{90}\text{Sr}]$ of about 10^{-10} M. For congruent release of Sr and U, the initial release of U must have been about 2.5×10^{-7} M; however, the $[\text{U}]$ measured in the first samples for cycles 4, 5, and 6 are much less than this. This indicates that the U was probably released as a small initial pulse, probably occurring before the vessels were closed. After closing the vessels and applying H_2 gas pressure, the U probably immediately began to precipitate in response to the reducing conditions inside the pressure vessel. The continued release of Sr during the entire test cycle suggests that continued dissolution and reprecipitation of the the fuel is occurring, resulting in Sr release. This would mean that U is being dissolved and reprecipitated even as the $[\text{U}]$ is decreasing towards a solubility limit appropriate to the reducing conditions in the tests.

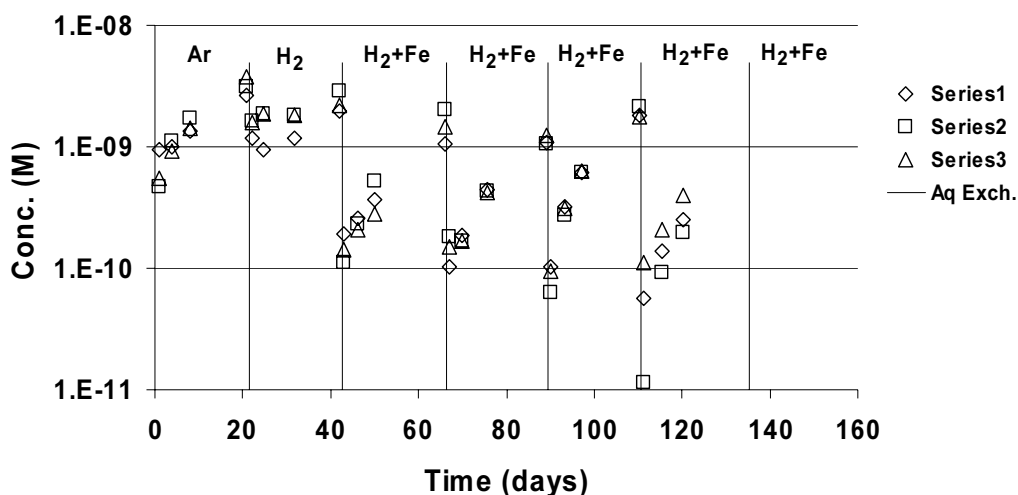


Figure 8. Leaching data for ^{90}Sr . Solvent extraction followed by Cerenkov counting of ^{90}Y .

At the end of this series of experiments the samples were left in their pressure vessels covered by modified Allard groundwater and with an atmosphere of 10 bar H_2 gas. Approximately 6 months later the isotope dilution experiments for the EU Project were started. The solution was removed from each test vessel and replaced with fresh modified Allard groundwater. The vessels were closed, the 10 bar H_2 gas atmosphere was added, and the samples were left for 2 weeks to equilibrate.

One of the difficulties in these tests is to find a way to introduce the spike solution without exposing the solutions to air. We decided to prepare a spike solution inside a pressure vessel so that the solution was under a H_2 gas atmosphere. The spike dose would then be applied by pushing the solution from the spike vessel to the sample vessel using gas pressure. Shortage of time meant that the spike concentration was too high at the time we needed to add it, leading to an overdose of spike. The composition of the spike was $^{234}\text{U} = 0.71 \pm 0.02\%$, $^{235}\text{U} = 84.6 \pm 0.1\%$, $^{236}\text{U} = 5.14 \pm 0.05\%$, $^{238}\text{U} = 9.53 \pm 0.05\%$.

The overdose of spike gave a large increase in the total U in the test vessels. A sample was taken immediately after adding the spike (in practice, about 1 hour after spike addition). Further samples were taken after 1, 7, and 18 days of testing. The samples were analyzed for U isotopic composition and concentration by ICP-MS, for ^{90}Sr via solvent extraction followed by Cerenkov counting of Y daughter product /Ramebäck et al, 1995/, and for Cs using a HPGe-detector for gamma detection. Data for the solution analyses are in /Ollila et al, 2003/. Data for ^{235}U and ^{238}U are given in table 4.

Table 4. [^{235}U] and [^{238}U] in spent fuel samples after spike addition.

Time days	^{235}U , ppb Series 1	^{235}U , ppb Series 2	^{235}U , ppb Series 3	^{238}U , ppb Series 1	^{238}U , ppb Series 2	^{238}U , ppb Series 3
0	35.35	112.98	32.93	4.33	13.02	4.56
1	32.83	103.43	30.41	4.31	11.85	3.71
7	21.82	43.80	16.48	3.80	5.52	2.33
18	4.73	9.82	3.13	2.14	3.07	1.97

The [U] in the first sample (day 0) is dominated by the spike addition. We can calculate the amount of U in solution before the addition of the spike by using the measured amounts for [²³⁵U] and [²³⁸U]. For Series 1, the addition of 35.35 ppb of ²³⁵U would have been accompanied by 3.98 ppb of ²³⁸U. The measured [²³⁸U] was 4.33, so the [²³⁸U] in solution before spike addition was 0.35 ppb. Since the spent fuel U is 99% ²³⁸U, this is essentially the total [U] in solution before spike addition (1.5×10^{-9} M). A similar calculation for series 2 gives a starting concentration of 0.29 ppb and for series 3 gives 0.85 ppb. These starting concentrations are in agreement with measurements that showed less than 1ppb in solution before spike addition.

All three samples show a relatively rapid decrease in [²³⁵U] and [²³⁶U] and a less rapid decrease in [²³⁸U]. This indicates that the spike over-dose is precipitating from solution, but at the same time, the spent fuel is continuing to contribute ²³⁸U to the solution phase. We can use the data from day1, day 7 and day 18 samples to estimate how much additional U has dissolved from the solid while the samples were being tested. The ratio of measured [²³⁵U] in the day 1 sample to that in the day 0 sample gives the amount of U left in solution. For series 1 there is 93% left in solution, for series 2, 92% and for series 3, 92%. If we use these estimates of precipitation to adjust the day 0 value for [²³⁸U], we estimate that the series 1 sample should have 4.02 ppb for [²³⁸U]. The measured value was 4.31 ppb, indicating that 0.29 ppb has been added to solution. Actually, the real addition would be somewhat greater since the sample is probably dissolving at a linear rate and precipitating at the same time, so some of the newly dissolved U has already precipitated when we take the day 1 sample. Since the amount of precipitation between day 0 and day 1 was only about 8%, the correction for the precipitation of newly dissolved U is small. It will be significant, however, for the later samples.

Between day 0 and day 7, the series 1 sample shows a decrease in [²³⁵U] from 35.35 ppb to 21.82 ppb. Thus, only 62% of the spike is left in solution. Of the original 4.33 ppb of ²³⁸U, only 2.67 ppb should be left. The measured [²³⁸U] is 3.80 ppb, so 1.13 ppb of this represents new U that has been added to solution by dissolution. If we assume that the precipitation rate was linear, this would be 80% of the amount that actually dissolved, giving a total amount of U dissolution of about 1.4 ppb, or 0.2 ppb per day. Comparison of the day 7 and day 18 data for [²³⁵U] shows that only 22% of the spike U present at day 7 is still in solution at day 18. Adjusting the day 7 [²³⁸U] for precipitation gives an expected value of 0.82 ppb if no dissolution occurred. The measured value was 2.14 ppb, indicating 1.32 ppb new U in solution. Comparison of the precipitation rate for day 0 to day 7 with that for day 7 to day 18 suggests that the precipitation rate is somewhat faster than linear. We estimate that the measured increase in [²³⁸U] would be about half of what actually dissolved, so total dissolution is about 2.6 ppb. Table 5 summarises calculations for all three sample series. The results are in quite good agreement and indicate an average dissolution rate of 0.2 to 0.3 ppb per day.

Table 5. Estimate of dissolution rate for spent fuel samples, ppb U.

Time interval	Series 1	Series 2	Series 3
Day 1 – day 0	0.3	nm	nm
Day 7 – day 0	1.4	0.7	0.07
Day 18 – day 7	2.6	3.6	3

nm = not meaningful

Data for ^{137}Cs concentrations are given in table 6. The initial concentrations of 2 to 4×10^{-10} M are consistent with the data from the first sample for the last three cycles in our earlier series of experiments. The data for the day 18 sample, with values between 6×10^{-10} M and 2×10^{-9} M, are considerably lower than the concentrations measured at the end of the leaching cycle in the previous tests.

The abundance of ^{137}Cs in the spent fuel is about 0.09% of the [^{238}U]. If U were dissolving from the fuel at the same rate as ^{137}Cs , we would expect the dissolution of U between days 7 to 18 to be between $(3 \times 10^{-10})/0.0009$ moles/L (sample 2) and $(1.4 \times 10^{-9})/0.0009$ moles/L (sample 3). This would give dissolution of 3×10^{-7} to 1.5×10^{-6} moles/L. The estimated U dissolution for that time period based on isotopic data was about 3 ppb, or 3 $\mu\text{g/L}$, corresponding to 1.2×10^{-8} moles/L. This indicates that ^{137}Cs is being released at a rate that is 25 to 125 times faster than the rate of matrix dissolution. This shows that ^{137}Cs release is not limited by the rate of matrix dissolution at this time.

Data for ^{90}Sr are not yet available. They will be added to the report as soon as the analyses are complete. This will allow us evaluate whether ^{90}Sr can be used as an indicator of matrix dissolution rate in experiments that have not used the isotope dissolution method to get a measured dissolution rate.

Table 6. ^{137}Cs Concentration in moles per liter.

Time, days	sample 1	sample 2	sample 3
0.1	3.83E-10	1.70E-10	2.43E-10
1	3.49E-10	1.25E-10	2.87E-10
7	5.81E-10	2.71E-10	4.13E-10
18	1.13E-09	5.79E-10	1.82E-09

WP 4 and 5

Reduction and precipitation of U and Np

Alpha radiolysis could create locally oxidising conditions close to the fuel surface and oxidise the U(IV) in the uranium dioxide fuel to the more soluble U(VI) oxidation state. Furthermore, the solubility of U(VI) is enhanced in the presence of bicarbonate/carbonate by the formation of strong anionic uranyl carbonate complexes. This increase in solubility can amount to 4 to 5 orders of magnitude depending on the composition of the groundwater in contact with the fuel. The other tetravalent actinides in the fuel, Np and Pu, also have higher solubilities when oxidised beyond 4+ to neptunyl and plutonyl species.

Once these actinides have been mobilised through oxidation, they can migrate away from this potentially oxidising region and will encounter an oxygen free, reducing environment caused by the anaerobic corrosion of the cast iron insert. The actinyl species are no longer thermodynamically stable and reduction to the tetravalent state will be possible. There is, however, an open question whether the reduction kinetics will be sufficiently high to cause reduction in solution and if sorption onto the corroding iron surface will be accompanied by an electron transfer sufficiently rapid to reduce the actinide back to the tetravalent state.

WP 4 and 5 consisted of experimental studies of uranium reduction-depletion from water solutions in the presence of corroding iron and of spectroscopic studies using resonant inelastic soft x-ray scattering (RIXS) spectroscopy of the oxidation state of uranium and neptunium sorbed/precipitated onto iron under oxygen free conditions. The details of these experiments are contained in /Butorin et al, 2003/.

The U samples used in RIXS studies were prepared at VTT. Iron foils were polished on one side with diamond spray (1 and 1/4 μm). An aliquot of U(VI) was added in the form of uranyl nitrate solution to deaerated modified Allard groundwater (100 ml) in a polyethylene bottle under N_2 atmosphere in a glove box. The composition of the Allard water is given in table 2 (WP1). The solution was allowed to equilibrate for a couple of hours. The starting concentration of uranium was about 500 ppb. At this uranium concentration, the dominant uranium species in solution are calculated to be $\text{UO}_2(\text{CO}_3)_3^{4-}$ (70%) and $\text{UO}_2(\text{CO}_3)_2^{2-}$ (25%). After equilibration, the Fe foils (2 pieces: 2 x 3 cm) were immersed in the solution in the bottle. The foils were placed on a small supporter (Teflon) the polished side upward. The experimental vessel was then allowed to stay tightly closed in the glove box.

The total U concentration in the solution was measured as a function of time with ICP-MS. The samples were not filtered. The redox potential (Eh) was measured after the experimental time of 40 days with a gold electrode and a Ag/AgCl/3M KCl electrode as the reference.

There was a rapid decrease in U concentration, see figure 9. A black 'deposit' was observed on the surface of the Fe foils after 3–4 weeks.

The measured redox potential in the solution at the end of the experimental period of 35 days was low, $E_h = -450$ mV.

The Fe foils that were sent for RIXS analyses had a reaction time of 17 days and 8.5 months. The U concentration in solution for the 17 days sample was 2.6×10^{-9} M. For the longer contact time, U concentration in solution was 1.5×10^{-10} M. The amount of black 'deposit' layer had increased.

Neptunium samples were prepared at Chalmers. The iron plates, about 1 cm^2 in size, were glued to a PEEK plate using either epoxy glue or silicon glue in order to avoid radioactive contamination on the reverse side of the iron plate. The plates were put in PEEK-lined steel vessels that can function with an overpressure of gas inside, referred to as pressure vessels in this report. Approximately 50 Bq of pentavalent neptunium was added to 20 ml of Allard water. The resulting starting concentration of neptunium in solution was approximately 4×10^{-7} M. Before the start of the exposure, the solution and the pressure vessel were purged with hydrogen gas. After sealing the vessel, an overpressure of 50 bar of hydrogen gas was applied. The neptunium concentration in solution was monitored every week and after four weeks, when the residual amount was less than 1% (no measurable Np in solution), the iron plates were removed.

The dominating neptunium species in the starting solution are calculated to be $\text{NpO}_2\text{CO}_3^-$ (75%) and NpO_2^+ (25%).

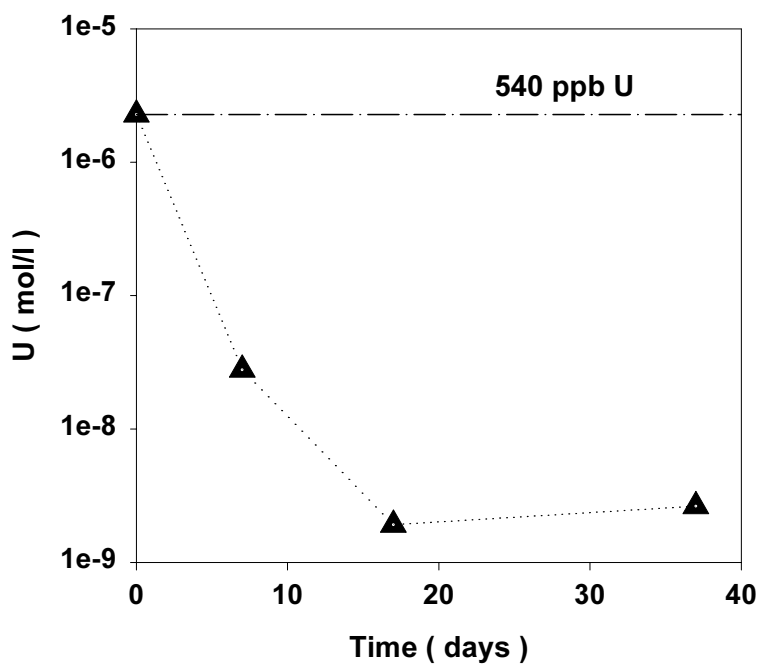


Figure 9. U concentration in Allard groundwater in the presence of metallic iron (Fe foils).

RIXS measurements

Most of the RIXS measurements were performed at the Advanced Light Source at Lawrence Berkeley National Laboratory, USA. For the study of uranium, some measurements were also performed at the MAX-lab, Lund University, Lund, Sweden.

RIXS measurements at the U 5d threshold provide an opportunity to study in detail elementary excitations in U compounds due to the higher resolution of such experiments in comparison with those at the U 3d and 4d thresholds /Butorin, 2000/. It has turned out that the technique is very sensitive to the valency and the chemical state of uranium in contrast to x-ray absorption spectroscopy (XAS). The 5d core-hole lifetime broadening is quite large, thus reducing the utility of XAS. In particular, it is difficult to distinguish between uranium species with different oxidation states, especially in the case when one of species has a much lower concentration than the other. In this situation, the virtually unlimited resolution (defined by the response function of the instrument) of the RIXS technique and its ability to enhance transitions to low-lying excited states are especially useful. RIXS spectroscopy provides good signatures in terms of new distinct transitions, representing electronic excitations within the 5f shell and having a characteristic profile for U(IV). The same kind of RIXS measurements were also made on the Np-on-Fe sample. The spectra were recorded at energies of the incident photon beam set to the pre-threshold structure in the Np 5d x-ray absorption spectrum.

The experiments were performed at undulator beamline 7.0 of the Advanced Light Source (ALS), LBNL, employing a spherical grating monochromator /Kalkowski et al, 1987/. Resonant ultra-soft x-ray scattering spectra from the samples were recorded using a grazing-incidence grating spectrometer /Warwick et al, 1995/ with a two-dimensional detector. The incidence angle of the photon beam was approximately 15° from the sample surface and the spectrometer was placed in the horizontal plane at an angle of 90° with respect to the incidence beam. The bandwidth of the excitation was about 65 meV. The total energy resolution of the RIXS data was estimated from the full width at half maximum of the elastic peak to be 160 meV.

Previous measurements on a set of uranium compounds and companion model calculations /Kalkowski et al, 1987/ showed that setting the energy of the incident beam close to the U 5d thresholds enhances the inelastic scattering cross section and ensures that electronic states of 5f symmetry are probed according to dipole selection rules. The spectral contribution of intra-ionic f-f transitions of U is enhanced at excitation energies close to 100 eV. At higher energies of the incident photon beam set to the main 5d absorption edge (e.g. 115 eV), inter-ionic excitations of charge-transfer character, such as ligand 2p – U 5f charge-transfer, dominate the RIXS spectra. The spectral pattern of intra-ionic f-f excitations is mainly determined by the formal valency of U. The charge-transfer transitions strongly depend on the chemical environment of U ions.

Figure 10 displays a set of scattering data from the Fe sample with 17-day exposure recorded at the incident x-ray energy of 100 eV, which corresponds to the energy of the weak pre-threshold structure in the U 5d x-ray absorption spectrum. A series of spectra were randomly measured from different 1 mm x 150 μm areas on the Fe sample surface. Six of them are shown in the figure along with spectra of the reference oxides UO₂ and UO₃ that contain U(IV) and U(VI), respectively. The choice of the excitation energy is defined by the necessity to selectively look at the intra-ionic f-f transitions.

An inspection of figure 10 shows the presence of two distinct RIXS structures at energy losses of about -0.8 and -1.15 eV in the UO_2 spectrum. These structures represent f-f transitions as incident x-rays are inelastically scattered on electronic excitations within the 5f shell. The structures are very well reproduced by model calculations of RIXS spectra using atomic multiplet theory for the U(IV) ion. Naturally, these structures are absent in the UO_3 spectrum due to the formal $5f^0$ configuration of the U(VI) ions. In this situation, any reduction of U(VI) on the Fe surface should result in the appearance of characteristic RIXS structures. The present measurements indeed reveal the presence of significant inelastic contribution in spectra recorded from some areas (spectra #4-6) on the surface of the Fe sample, thus indicating U(VI) reduction in those areas.

A comparison of RIXS spectra of the charge-transfer transitions between the foil and UO_2 , made in figure 11, suggests that U(IV) species on the Fe foil are not necessarily in the form of uranium dioxide. The RIXS profiles of compared spectra are somewhat different. Similar results were obtained for another Fe foil prepared under the same conditions but with much longer exposure (8.5 month) to the U(VI) solution.

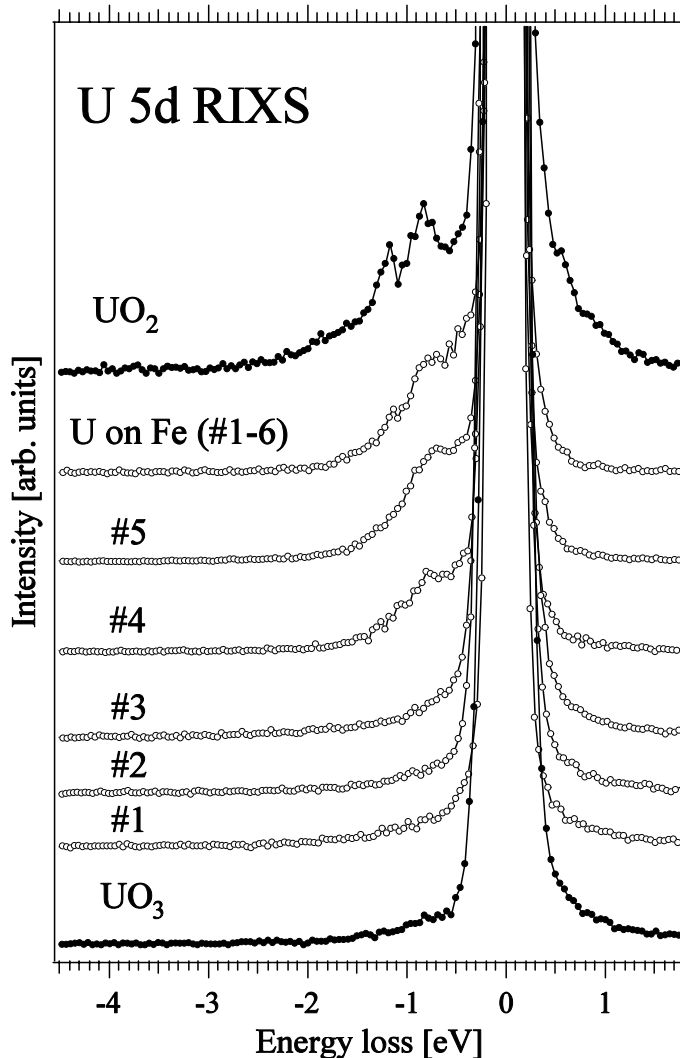


Figure 10. Enhanced inelastic part of soft x-ray scattering spectra of UO_2 , UO_3 and U adsorbed on the Fe foil (elastic peaks are at 0 eV). The energy of the incident photons was set to 100 eV. The six spectra of adsorbed U were randomly measured from different $1\text{mm} \times 150\ \mu\text{m}$ areas on the surface of the Fe sample.

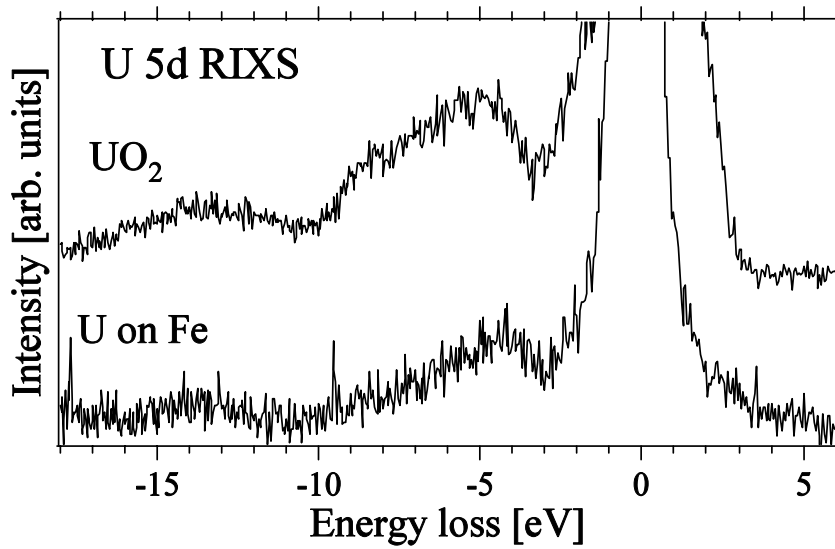


Figure 11. Enhanced inelastic part of the soft x-ray scattering spectra of UO_2 and U adsorbed on the Fe foil recorded at the excitation energy of 115.0 eV.

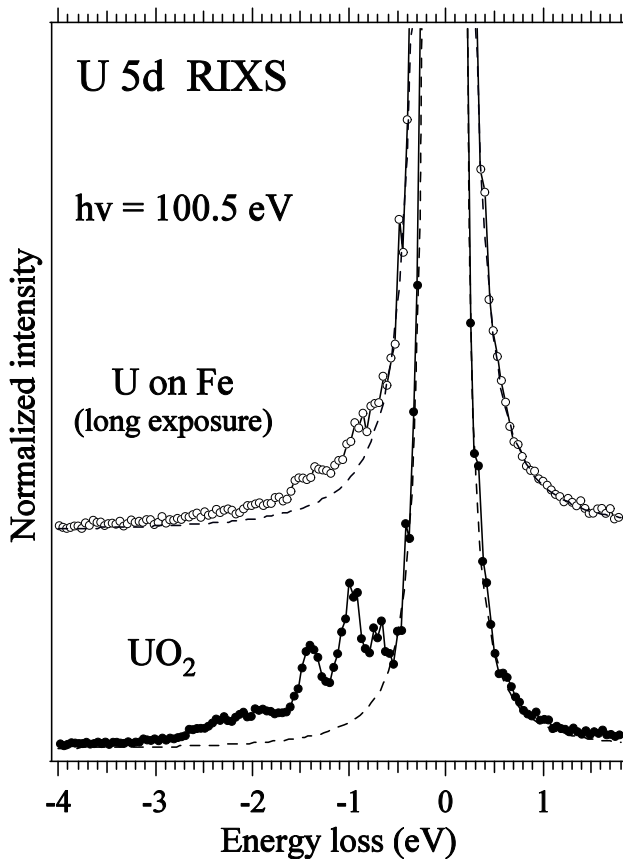


Figure 12. Enhanced inelastic part representing f - f excitations in the soft x-ray scattering spectra of single-crystal UO_2 and U on the long-exposure Fe sample. Dashed lines represent Voigt fits of the elastic peaks.

Quantitative estimates of the amount of reduced uranium were made by normalising the recorded spectra to the characteristic core-to-core fluorescence lines and by comparison to model oxide systems with well-defined oxidation states for uranium. Using UO_2 single crystal standards, we were able to compare the recorded spectra from the standards and the samples described above after normalisation to the non-resonant U 6p-to-5d fluorescence line recorded with excitation above the 5d edge. An example of such a comparison is shown in figure 12. By fitting the elastic peak with the Voigt profile and estimating the area under the spectral curve in the energy-loss range corresponding to the f-f transitions the amount of reduced uranium can be derived. In this manner, we could estimate that 73% of the total uranium on the foil from the 17 days experiment is in fact present as U(IV) and for the 8.5 months experiment 42% was present as U(IV) taking into account the spatial heterogeneity. The reason for this reversed behaviour may be possible peeling off of layers of the U(IV) compound.

Figure 13 shows a number of RIXS spectra of NpO_2 used as reference system for the tetravalent oxidation state for Np. The spectra were recorded at energies of the incident photon beam set to the pre-threshold structure in the Np 5d x-ray absorption spectrum. (The top figure in figure 13.) At such energies, the x-ray scattering cross-section is enhanced for f-f transitions. The excitation energies for the spectra are indicated in the figure with the letters a, b, c, and d. The energy losses of the corresponding RIXS structures observed in figure 13 are in agreement with optical absorption measurements of f-f transitions in Np(IV) systems /Gruber and Menzel, 1969; Jørgensen, 1955/.

The spectra in figure 13 are compared with the results from atomic multiplet calculations for the Np(IV) ion. The calculations were performed in a similar manner as was described for the case of U(IV) in the previous section, only this time the $F^k(5f; 5f)$ integrals were scaled down to 70%. The initial and final states of the scattering process were taken to be those of the $5f^3$ configuration with the intermediate states of $5d^p5f^4$ character which are mainly autoionised to $5f^2eg$ states. The calculated spectra show slight differences in the energy position for some RIXS structures when compared with the experimental spectra. This is likely due to the influence of the crystal field interaction and/or the Np 5f-O 2p hybridisation, which were not taken into account in the calculations. The extra-structure observed in the experimental spectra at an energy loss of around 950 meV may also be a result of the crystal field interaction. Nevertheless, the present calculations account for the overall RIXS profile and behaviour and reproduce its dependence on the excitation energy.

Figure 14 displays RIXS spectra of Np sorbed on the Fe stripe along with NpO_2 spectra recorded at the same excitation energies. An inspection of this figure shows that the RIXS structures of both samples closely resemble each other. This resemblance unambiguously indicates the existence of Np in the form of Np(IV) on the studied Fe stripe.

RIXS spectra of the charge-transfer transitions between the foil and NpO_2 are shown in figure 15. The corresponding spectra for uranium suggested that U(IV) species on the Fe foil is not necessarily in the form of uranium dioxide. The RIXS profiles of NpO_2 and neptunium on the iron are much more similar, indicating the Np(IV) species is likely to be NpO_2 .

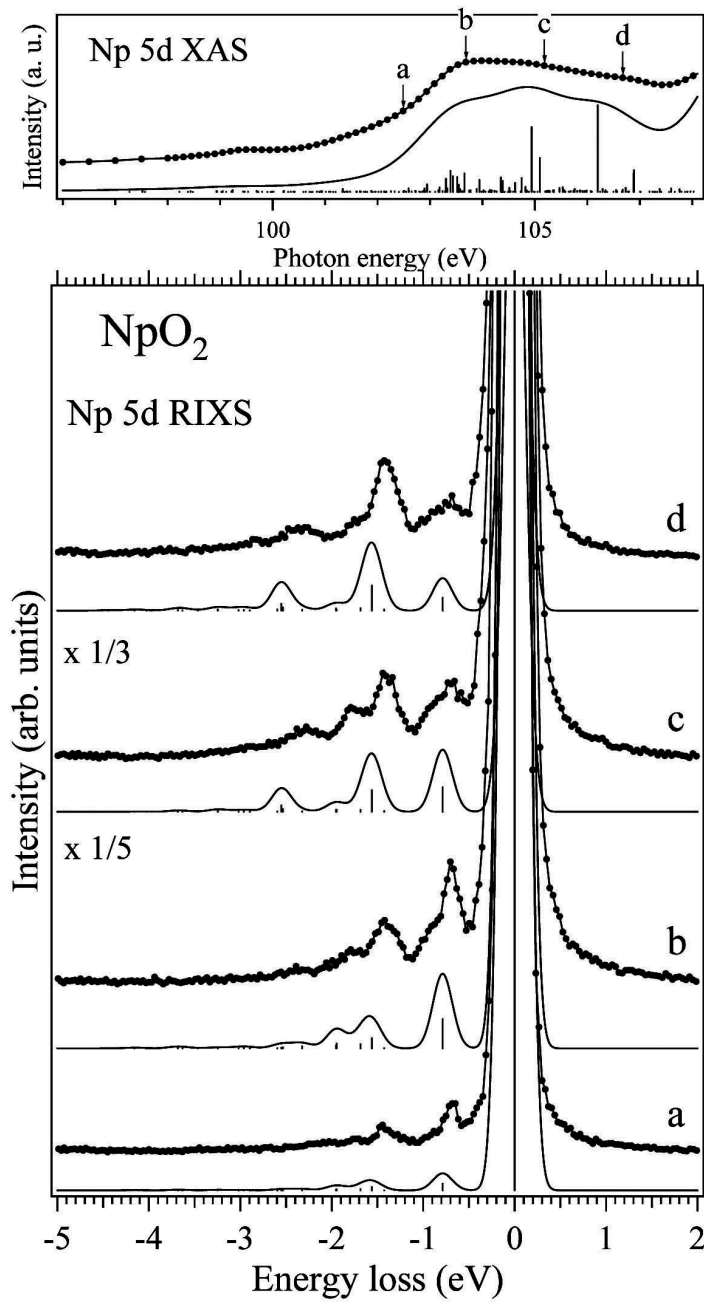


Figure 13. Resonant x-ray scattering spectra of NpO_2 recorded at different excitation energies close to the Np 5d threshold (lines with markers) together with the results of atomic multiplet calculations (sticks with thin lines) for the Np^{4+} ion. Excitation energies are indicated by arrows on the total electron yield spectrum at the Np 5d absorption edge shown in the top panel.

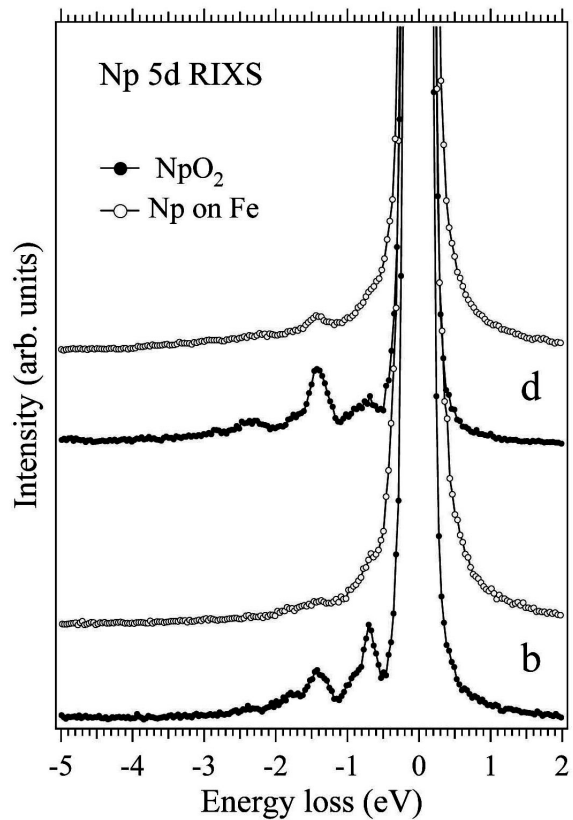


Figure 14. Comparison of resonant inelastic soft x-ray scattering spectra of Np sorbed on the Fe stripe and NpO_2 . Letters correspond to the same excitation energies as in figure 13.

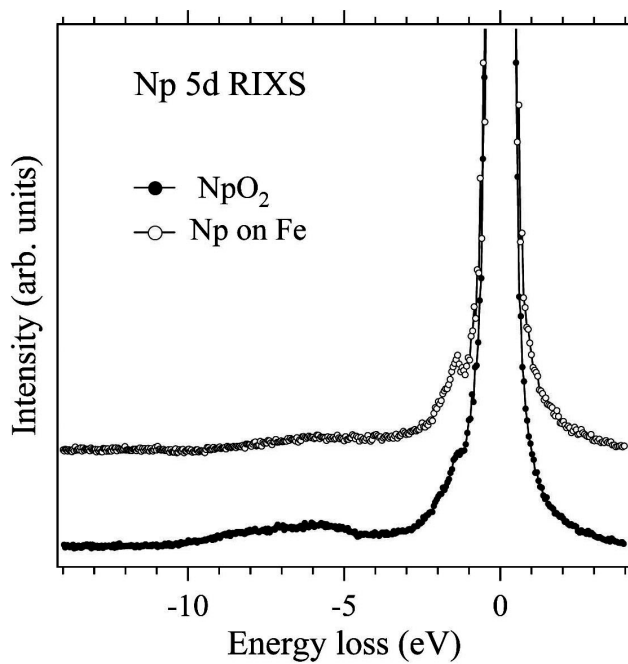


Figure 15. RIXS spectra of the charge-transfer transitions between the iron foil and NpO_2 .

Chemical and electrochemical measurements

The species to be studied were U(VI) carbonates and U(VI) hydroxides. The solution for U(VI) carbonate complexes was a NaCl-NaHCO₃ solution. The dominant species under these conditions are UO₂(CO₃)₃⁴⁻ (63%) and UO₂(CO₃)₂²⁻ (24%). The NaCl-NaHCO₃ had an ionic strength (I = 0.003) and bicarbonate content (1.1 mM) similar to Allard groundwater. The U(VI) was added to solution as an aliquot of uranyl nitrate solution (UO₂(NO₃)₂ × 6 H₂O).

The solution for U(VI) hydroxide complexes was 0.1 M NaCl with high pH. The dominant species is UO₂(OH)₃⁻ (99%).

Reduction tests were performed in the active corrosion cell under anaerobic conditions in the glove box (N₂). The cell was made of glass. It had an inner vessel made of polyethylene. Iron strips were immersed in deaerated U(VI) solution in the cell. The evolution of uranium concentration was followed versus reaction time with periodic sampling through the sampling port for further analysis of uranium (ICP-MS). The oxidation state of uranium in solution was analysed in selected tests using a method that is based on the separation of the tetravalent and hexavalent states by anion-exchange chromatography in HCl medium. The analyses of the U contents of each of the fractions were measured by ICP-MS. The method is described in detail in /Ollila, 1996/.

The cell had electrodes for the in-situ monitoring of pH, E_h and corrosion potential of iron during reduction reaction /Peat et al, 2001/:

- palladium black electrode (hydrogen electrode) for pH
- gold electrode for E_h
- iron electrode for corrosion potential
- silver-silver chloride electrode as reference

The Fe electrode was made of iron metal of the same composition as the iron strips that were used as reducing agent in the aqueous phase.

The functioning of the pH and the reference Ag/AgCl electrodes caused problems in the preliminary measurements in NaCl-NaHCO₃. The potential values of all three electrodes changed from negative to positive 85 minutes after the start of a reduction test, figure 16. Since the potential values changed simultaneously it was concluded that it was the potential of the reference electrode that had changed. After the test, the potential of the Ag/AgCl electrode was measured versus a commercial calomel electrode. The reading was not stable. One possible reason for failure could be the dissolution or cracking of the silver chloride coating of the electrode in the test solution that contained chloride ions. The lifetime of the Pd black electrode proved to be short, 4–5 days after the electrolysis, under anaerobic conditions.

After that, the reference and pH electrodes were replaced with commercial electrodes (Innovative Instruments, Inc., USA), which were made suitable for the corrosion cell. The leak-free Ag/AgCl reference electrode was constructed from PEEK. The filling electrolyte was 3.4 M KCl. The electrode has a junction that is highly conductive but not porous. The pH sensitive tube with a metal-metal oxide pH sensing mechanism was also constructed from PEEK.

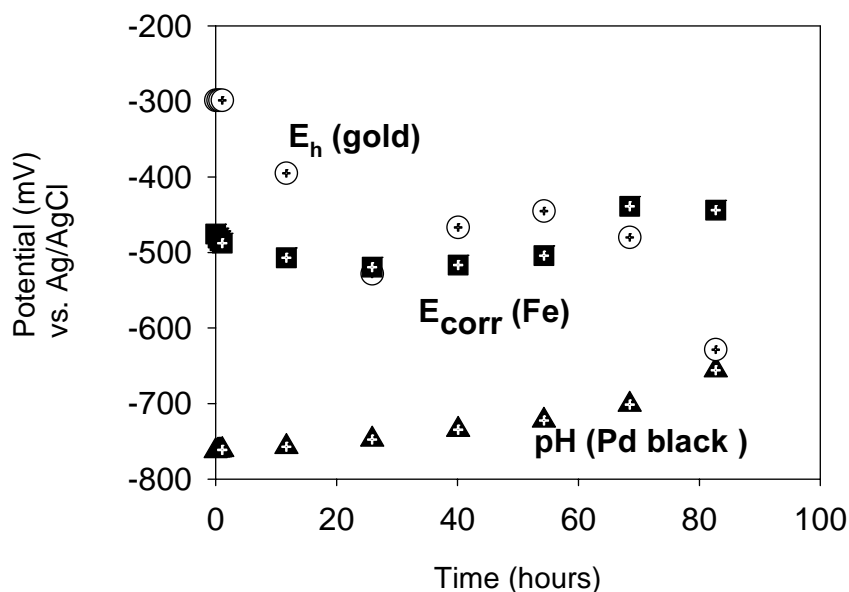


Figure 16. Potential of pH, gold and Fe electrodes in a preliminary U reduction test in NaCl-NaHCO₃ solution (25 °C).

The RIXS measurements show that at least partial reduction of both uranyl carbonate complexes and neptunyl carbonate complexes take place on the corroding iron surface.

The chemical/electrochemical measurements indicate that reduction of uranyl carbonate complexes also takes place in solution in a system containing corroding iron: i.e., sorption onto the iron/iron oxide surface may not be necessary in order for reduction to take place. Reduction of uranyl hydroxyl complexes was also found to take place in solution, but at a rate that was noticeably lower than for the uranyl carbonate complexes.

Two parallel reduction tests (Test I, II) were performed in NaCl - NaHCO₃ solution. The conditions are given in table 7. The amount of iron was different in the tests. Otherwise the conditions were similar. The iron strips were transferred to the test solution one day before the U addition. The temperature in the glove box was 30 °C instead of the normal 25 °C during these tests due to the breakdown of the cooling system of the box.

The results of monitoring the pH, Eh and corrosion potential of iron in NaCl-NaHCO₃ in the presence of iron strips during the first 17 hours are shown in /Butorin et al, 2003/. The pH behaved somewhat differently in the tests. It is not known if this was dependent on the calibration of the electrode. The pH in Test I (about 7.0) seems too low. The final

Table 7. Conditions of the reduction tests.

	Initial U (ppb)	Solution (ml)	Initial pH	Fe SA/solution V
Test I	560	300	8.7	19 cm ² /300 ml
Test II	500	250	8.7	38 cm ² /250 ml

pH (9.1) in Test II is in agreement with the measurements done in WP1 tests in Allard groundwater. The E_h had decreased to around -400 mV due to the anaerobic corrosion of the iron surface, leading to the release of Fe^{2+} -ions to the solution. It was 50 mV lower at the end of the measurement period in Test II that had a higher ratio of the Fe surface to solution volume. There was some disturbance at the early stage of the measurement in Test II. The corrosion potential of iron stabilised in 3–4 hours at -530 mV.

After the addition of the U(VI) as an aliquot of uranyl nitrate solution the pH decreased slowly in Test I and more rapidly in Test II. There was a small initial increase in Test I from 8.3 to 8.5. The pH started to increase again after 5 hours in Test II with more metallic iron. The E_h of the solution increased rapidly after the uranyl, UO_2^{2+} , addition. The reaction seemed to be very fast in Test II. At the later stages the E_h decreased to the original level again. The initial increase suggests the reaction between Fe^{2+} and U(VI)-carbonate complexes in solution, leading to the oxidation of Fe^{2+} . An attempt was made to analyse the oxidation state of the U in solution in Test I. The samples for the analyses were taken 3, 27 and 49 hours after the U addition.

The results, table 8 showed the presence of the U at the tetravalent state in solution. This suggests the reduction of U to take place in solution. The corrosion potential of the iron electrode remained approximately at the same level as before the U addition.

The evolution of the total U contents in test I showed a rapid decrease in U concentration during the first five hours after the U addition, which was followed by a slower decrease. The U decreased from 560 to 150 ppb with the reaction time of 55 hours under these conditions. In test II, the decrease was much faster, probably due to the larger amount of metallic iron, table 7. The U decreased to 0.02 ppb (8.4×10^{-11} M), the detection limit of U by ICP-MS, by the reaction time of 24 hours. This U level is in agreement with the U concentrations measured in the isotope dilution tests of WP1 and WP2.

The reduction tests in 0.1 M NaCl (pH 11) were performed in the active corrosion cell as were the tests in NaCl- $NaHCO_3$. The pH of the deaerated 0.1 M NaCl solution was adjusted to 11 with 0.1 M NaOH. The solution was allowed to equilibrate with the iron strips for one day before the U addition. The temperature in the glove box was 25 °C during these tests. Two parallel tests were performed, table 9.

Table 8. Results for U oxidation state in solution.

Samples	U(IV) %	U(VI) %
3 hours	16	84
27 hours	51	49
49 hours	53	47

Table 9. Conditions of the reduction tests in 0.1 M NaCl.

	Initial U (ppb)	Solution(ml)	Initial pH	Fe SA/V
Test III, IV	500	250	11.0	28 cm ² /200 ml

The pH electrode of the corrosion cell showed some inconsistency in the measurements. The pH decreased slowly in both tests. The pH was checked with a Ross combination glass pH electrode at the end of the equilibration periods with iron strips by taking samples for measurements. According to these measurements, the pH had not changed from the original value of pH 11 in either of the tests. The potentials of gold and iron stabilised rapidly at low levels after the addition of the iron strips.

After the addition of the U(VI) as an aliquot of uranyl nitrate solution, the continuous pH measurement in the reaction cell gave a falling value up to the end of the experimental time. This is in disagreement with the results of the parallel test IV. In this case the pH was measured with a micro-combination glass pH electrode by taking samples from the reaction cell. The measurements did not show any change in pH. The pH measurement with the Ross glass pH electrode at the end of the Test III gave also the original value of 11. It is probable that the pH does not change during the tests.

The Eh increased in Test III rapidly after the U addition from the level before the addition (~ -460 mV) and stayed higher after that suggesting the reaction between Fe^{2+} in solution and U(VI)-hydroxide complexes. There were disturbances in the measurement at the early stages of the test. The Eh decreased to the original level afterwards, in agreement with the reduction tests of uranyl carbonate. The parallel test gave a different result. The E_h stayed at the higher level to the end of the experimental time. The corrosion potential of iron did not change after the U addition in the tests.

The evolutions of the total U contents are shown in figure 17. The test IV was continued for a longer period (8 days) in order to see the final U concentration. The U concentration decreased from 500 to 20 ppb in the presence of iron strips. The oxidation state of U was analysed in Test III. The samples were taken 2.5, 28 and 74 hours after the U addition. The amount of the U at the tetravalent state was lower than in the reduction tests I and II, see table 10.

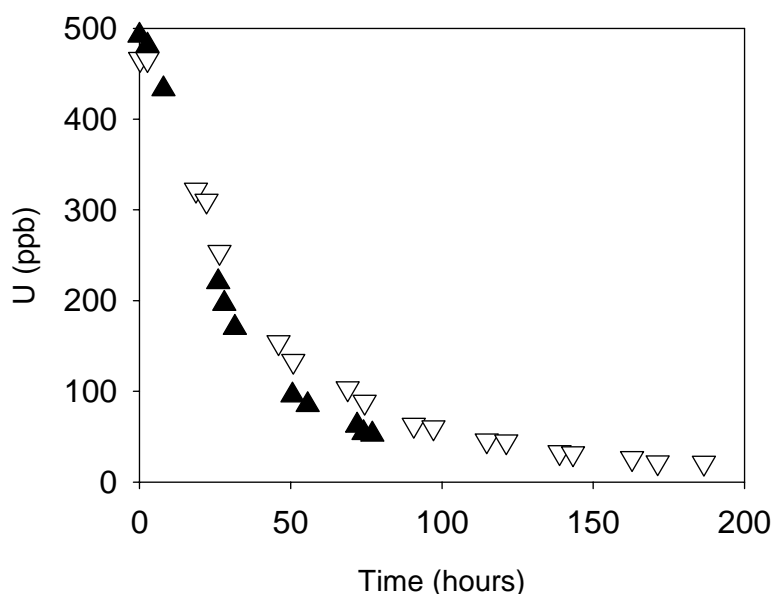


Figure 17. Total U concentration (ppb) in Test III (black symbols) and Test IV (open symbols) after the addition of U to 0.1 M NaCl (initial pH 11) in the presence of iron strips (25°C).

Table 10. Results for U oxidation state in solution.

Samples	U(IV) %	U(VI) %
2.5 hours	4	96
28 hours	12	88
74 hours	14	86

WP 6

Thermodynamics of the reduction of U(VI) to U(V) by Fe(II)

In the present work, we have addressed an important redox reaction, the reduction of U(VI) to U(V) in the presence of Fe(II). Redox reactions are not only of fundamental interest, to understand them is essential when describing how chemical reactions of actinides in surface and groundwater systems affect their mobility in the biosphere, and the function of engineered systems for the containment of radioactive waste in underground repositories. In this context it is important to notice that spent nuclear fuel is predominantly a matrix of UO_2 in which fission products and higher actinides are dispersed. In contact with water the fuel matrix will dissolve with a resulting release of the different radionuclides; the dissolution is a result of oxidation by radiolysis products or by intruding oxygen. In most technical system the nuclear waste is contained in canisters of iron/steel, which provide a large reduction capacity to the system and thus may prevent the transformation of sparingly soluble UO_2 to more soluble U(VI) species. Corrosion and other redox reactions involving iron species are therefore of key importance for the safe performance of many nuclear waste installations; as these have to function over very long time periods it is highly desirable to base predictions of their future environmental effects on molecular understanding of the chemical reactions taking place.

During the first phase of the project we investigated the thermodynamics of the reduction of U(VI) to U(V) by Fe(II) using *ab initio* methods. Our analyses are, in accordance with experimental information, based on the thermodynamics of the precursor and successor complexes formed before and after the electron transfer between uranium and iron. Experiments show that the rate of electron transfer is highly variable, but the detailed mechanisms of reactions involving actinides are very incompletely known. The overall stoichiometry of the reduction of U(VI) to U(V) by Fe(II) in water solution at different pH may be written as



where $p + q = r + s = n = 4, 5, 6$, and the larger values of n present at higher pH. At low pH the first co-ordination shell consists mainly of water molecules that are replaced by hydroxide ions at higher pH. Eq. (1) describes the stoichiometry of the redox reaction; the mechanism of the reaction is more complex (and largely unknown) and involves several steps. We explored an inner-sphere pathway involving two hydroxide bridges between iron(II) and uranium(VI) in the precursor complex and between iron(III) and uranium(V) in the successor complex. The latter is subsequently reduced to U(IV) and/or disproportionates according to



The over-all reduction of U(VI) to U(IV) by Fe(II) in solution is slow, presumably due to a slow reduction of U(V) to U(IV).

The focus of the study was on the reduction to U(V) as shown in eq. 3.



As this reaction involves the transfer of only one electron and minor rearrangements in the coordination spheres between U(VI) and U(V) we expect the reaction to be faster than the following reduction to U(IV). We have used different quantum chemical methods to determine the geometry and relative energy of different U(VI)/Fe(II) precursor and U(V)/Fe(III) successor complexes and the change in total energy during the reaction. U(VI) on the left hand side of reaction (3) is a closed shell system while Fe(II) has four open *d*-shells; on the right hand side of the reaction there is one open *f*-shell on U(V) and five open *d*-orbitals on Fe(III). We have assumed that the reduction of U(VI) and the simultaneous oxidation of Fe(II) take place through electron transfer from the iron *d*-shell into the empty *5f*-shell of uranium, via bridging hydroxide ligands.

A general problem with actinides is the need to take the strong relativistic effects, the semi-core character of the *6s* and *6p* shells and the active role played by the *5f*-orbitals, into account. The large number of electrons, which must be treated explicitly in the calculations, restricts the number of atoms that can be included in the model. Another problem, specific for the present study, is the open *d*-shells on Fe(II) and Fe(III). The large number of both doubly occupied orbitals and unpaired electrons makes the calculations technically demanding and, in particular, the correlation treatment becomes cumbersome. The net effect is that the calculations become very complicated. The reaction was studied in solution; solvent effects were included by the polarizable continuum model (PCM). The U(VI)-Fe(II) and U(V)-Fe(III) complexes contain double hydroxide bridges, both in solution and in the gas phase. Experimentally the reaction is endothermic at low pH and exothermic at high pH.

According to our calculations the reaction is thermo-neutral or slightly exothermic for five and six hydroxide ligands, in agreement with observations, but exothermic with four hydroxides. The solvent effects were appreciable, of the order of 50 kJ/mol on the reaction energies in the case of four hydroxide ligands. The PCM model is, although often satisfactory, not a highly precise model, and the description of the solvent had to be improved. The complexity of the calculations only allowed us to add two extra water molecules to the four-hydroxide complex. As a result of this the PCM effect decreased to about 10 kJ/mol, and the results seemed more or less stable. We, thus, have good reasons to believe that the solvent effects obtained with the PCM model overestimate the reaction energy, in particular in the four hydroxide complex, and that a better calculation would render the reaction endothermic. However, to add more water molecules to the complexes would make the calculations exceedingly difficult unless the computational model is simplified.

Our model is capable of reproducing experimental data reasonably well, but it is not possible to improve the solvent model by adding more water molecules, or to apply it to cases with larger ligands such as carbonate. The results of this study have been published in /Privalov et al, 2003a/.

The main problem in this study was the description of the unpaired *d*-electrons on iron, and the simplification we chose was to develop a model for the iron ion where the problematic *d*-electrons were described by a simple potential. The approach has previously proved successful in models describing chemisorption and reactions on nickel and copper surfaces developed in our group. /Dolg et al, 1989/ have used a similar concept for the lanthanides, where ECPs which include the *4f*-shell in the core have been quite successful. The *3d*-shell in Fe is more flexible than the *3d*-shell in the transition metals to the right in the periodic table and the *4f*-shell in the lanthanides, and

more apt to participate in chemical bonds. However, the complexes of interest to us are highly ionic, with quite localized 3d-shells on Fe, and we deemed it worth the effort to develop a one-electron ECP also for Fe. Another complication in the present case is that we study redox processes, and it is unlikely that one single ECP can describe both Fe(II) and Fe(III). We thus decided to develop two different one-electron ECPs, one for Fe(II) and one for Fe(III). This would allow us to investigate, for example, solvent effects for the precursor and successor states (Fe(II) and Fe(III)) separately.

In the second phase of the project we developed very-large-core (one-electron) ECPs, which include the d-electrons in the core, for Fe(II) and Fe(III). The previous study of uranium reduction by Fe(II) provided data (geometries and relative energies of precursor/successor uranyl-iron complexes with different ligand arrangements) which could be used to optimize the model potentials. In addition to the U-Fe complexes the model has been applied to hydrated Fe(II) and Fe(III). We have also calculated geometries and relative energies in some iron-containing enzymes (the non-heme Fe(II)/Fe(III) phenylelanine hydroxylase).

Since different potentials had to be used for different oxidation states of Fe, it would at first sight seem as if the results cannot be used to calculate redox reaction energies. However, it turned out that a simple atomic correction gives excellent results for reaction energies obtained at the SCF level. The results were encouraging; both geometries and relative energies between conformers are reproduced at least on a semi-quantative level. At the SCF level a correction factor that gives fairly accurate reaction energies can be obtained from atomic data, while at the MP2 level it seems necessary to use molecular data to deduce a correction factor. We are planning to pursue these studies in the future.

Geometries were reasonably well described in Fe(II)/Fe(III) phenylelanine hydroxylase, where the covalent interaction between the ligands and the metal is more pronounced than in the essentially ionic hydroxide complexes, while energy differences were less accurate. The approximation cannot be expected to work well for these systems where the d-orbitals participate directly in the bonding, but nevertheless we get reasonable geometries; in particular the topologies are correctly described, which is an encouraging result. This study has been submitted for publication in *J. Phys. Chem A* /Privalov et al, 2003b/.

References

Albinsson Y, Forsyth R, Skarnemark G, Skålberg M, Torstenfelt B and Werme L, 1990. In Sci. Basis for Nucl. Waste Management XIII, ed. V. M. Oversby and P. W. Brown (Mater. Res. Soc. Proc. 176, Pittsburgh, PA) pp. 559–565.

Albinsson Y, Ödegaard-Jensen A, Oversby V M and Werme L O, 2003. Leaching of spent fuel under Anaerobic and Reducing Conditions, in Sci. Basis for Nucl. Waste Management XXVI, D. Bullen and R. Finch, eds. (Mat. Res. Soc. Proc. XYZ, Warrendale, PA) in press.

Butorin S, Ollila K, Albinsson Y and Werme L, 2003. Reduction of Uranyl and Neptunyl Carbonate Complexes Studied with Chemical-Electrochemical Methods and RIXS Spectroscopy. SKB TR-03-15, Svensk Kärnbränslehantering AB.

Dolg M, Stoll H, Savin A, Preuß H, 1989. Energy-adjusted pseudopotentials for the rare earth elements, Theor. Chim. Acta 75, 369–387.

Gruber J B and Menzel E R, 1969. J. Chem. Phys. 50, 3772.

Jørgensen C K, 1955. J. Inorg. Nucl. Chem., 1 301.

Kalkowski G, Kaindl G, Brewer W D and Krone W, 1987. Phys. Rev. B35, 2667.

Kleykamp H, 1985. J. Nucl. Mater. 131, 221–246.

Ollila K, 1996. Determination of U oxidation state in anoxic (N₂) aqueous solutions – method development and testing, Helsinki, Finland: Posiva Oy. Posiva Report 96-01.

Ollila K, 1999. Dissolution of unirradiated UO₂ fuel in synthetic groundwater – Final report (1996–1998), Posiva 99-24, Posiva OY, Helsinki, Finland.

Ollila K, Albinsson Y, Oversby V and Cowper M, 2003. Dissolution rates of unirradiated UO₂, UO₂ doped with ²³³U, and spent fuel under normal atmospheric conditions and under reducing conditions using an isotope dilution method. SKB TR-03-13, Svensk Kärnbränslehantering AB.

Peat R, Brabon S and Smart N R, 2001. Design of Active Corrosion Cell, Serco Assurance Report SA/RJCB/62035/R01 Issue 1.

Privalov T, Schimmelpfennig B, Wahlgren U, Grenthe I, 2003a. Reduction of Uranyl(VI) by Iron(II) in Solutions: An Ab Initio Study, J. Phys. Chem. A 107, 587–592.

Privalov T, Schimmelpfennig B, Bassan A and Wahlgren U, 2003b. Reduction of uranyl(VI) by iron(II): application of a new Effective Core Potential for Fe(II) and Fe(III), submitted to J. Phys. Chem. A.

Ramebäck H, Albinsson Y, Skålberg M, Sätmark B and Liljenzin J O, 1995. Nuclear Instruments and Methods in Physics research, A357, 540–545.

Ramebäck H, Albinsson Y, Skålberg M and Werme L, 1994. Radiochimica Acta 66/67, 405–408.

Wahlgren U, 2003. Investigating the thermodynamics of the reduction of U(VI) to U(V) by Fe(II) using ab initio methods. SKB TR-03-14, Svensk Kärnbränslehantering AB.

Warwick T, Heimann P, Mossessian D, McKinney W and Padmore H, 1995. Rev. Sci. Instrum. 66, 2037.